Novel Index Modulation Aided Non-Orthogonal Multiple Access for Visible Light Communication

Tengjiao Wang[1], Fang Yang[1,2], Jian Song[1,2]
[1]Department of Electronic Engineering, Tsinghua University,
Beijing National Research Center for Information Science and Technology (BNRist), Beijing 100084, P. R. China
[2]Key Laboratory of Digital TV System of Guangdong Province and Shenzhen City,
Research Institute of Tsinghua University in Shenzhen, Shenzhen 518057, P. R. China
E-mail: wangtj16@mails.tsinghua.edu.cn, fangyang@tsinghua.edu.cn, jsong@tsinghua.edu.cn

***Abstract*—In this paper, a novel index modulation aided non-orthogonal multiple access (NOMA) scheme is proposed for visible light communication (VLC). Unlike the conventional NOMA schemes, the proposed scheme conveys information for different users through both the index-domain and constellation-domain symbols with the aid of index modulation, which is able to cancel the intra-cluster interference completely and avoid the use of successive interference cancellation to decrease computational complexity. The achievable multi-user sum rate of the proposed scheme is analyzed and a closed-form expression of the lower bound is derived. Then, an approximation is further obtained to realize accurate prediction of the achievable multi-user sum rate. Simulation results validate the accuracy of the approximation of the achievable sum rate and the superior performance of the proposed scheme.**

***Index Terms*—index modulation, non-orthogonal multiple access (NOMA), visible light communication, optical orthogonal frequency-division multiplexing, intra-cluster interference.**

I. Introduction

In recently years, with the rapid increase in the usage of light emitting diodes (LEDs) all over the world, visible light communication (VLC) has been emerging as one of the promising candidates to complement the radio frequency (RF) communication [1]. Since the LEDs can switch to different levels of light intensity at a very fast rate theoretically, which is imperceptible by a human eye, LEDs can be utilized to provide dual services of energy-efficient illumination and high-speed communication [2]. Starting from the beginning of the twenty-first century, VLC has attracted a tremendous amount of attention from both academia and industry, including resource allocation [3], dimming control [4], and hybrid systems [5].

In order to obtain high data rate and alleviate inter-symbol interference, optical orthogonal frequency division multiplexing (OFDM) is widely adopted in VLC [6]. Different from the conventional OFDM in RF communication, real-valued unipolar time-domain signals are required in optical OFDM to facilitate intensity modulation and direct detection (IM/DD) [7]. However, optical OFDM suffers from high peak-to-average power ratio (PAPR). Recently, index modulation is put forward to reduce PAPR and alleviate inter-carrier interference [8], where the information bits are mapped on both the conventional constellation and the indices of the activated subcarriers. By adjusting the number of activated subcarriers, index modulation can provide the trade-off between bit error rate and spectral efficiency [9].

In the downlink multi-user scenario for VLC, multiple access techniques are of great importance [10]. Non-orthogonal multiple access (NOMA), which allows the information intended for different users to be transmitted on non-orthogonal time-frequency resources, has been recognized as promising multiple access techniques for 5G and beyond 5G networks [11], [12]. Recently, NOMA has been introduced into VLC downlink and attracted considerable research efforts, including performance analysis [13], user grouping [14], power allocation [15], and so on. However, the complicated successive interference cancellation (SIC) is adopted in conventional NOMA schemes to alleviate intra-cluster interference between users, which is not friendly to the users with limited computing capacities, such as the Internet of Things (IoT) devices [16].

In this paper, we propose a novel index modulation aided NOMA (IM-NOMA) scheme for VLC. In the proposed scheme, the users are divided into clusters, where orthogonal resources are allocated among different user clusters and non-orthogonal resource allocation is adopted within each cluster. Specifically, the information for the users in different clusters are transmitted on orthogonal subcarriers, while the information for the users in the same cluster is transmitted on the same subcarrier group. The data information intended for different users is mapped on the index-domain symbols and the constellation-domain symbols respectively, thus the complicated signal processing caused by SIC is avoided. We analyze the achievable multi-user sum rate of the proposed IM-NOMA scheme and obtain the closed-form approximation through mutual information analysis. Numerical simulations are carried out to demonstrate the superior performance of the proposed scheme.

The rest of this paper is organized as follows. In Section II, the system model of the index modulation aided VLC system is introduced. In Section III, the proposed IM-NOMA scheme is explained in detail. The multi-user sum rate is also analyzed and a closed-form expression is derived. Then,

978-1-7281-0962-6/19/$31.00 ©2019 IEEE
Authorized licensed use limited to: Tsinghua University. Downloaded on September 27,2020 at 12:50:31 UTC from IEEE Xplore. Restrictions apply.

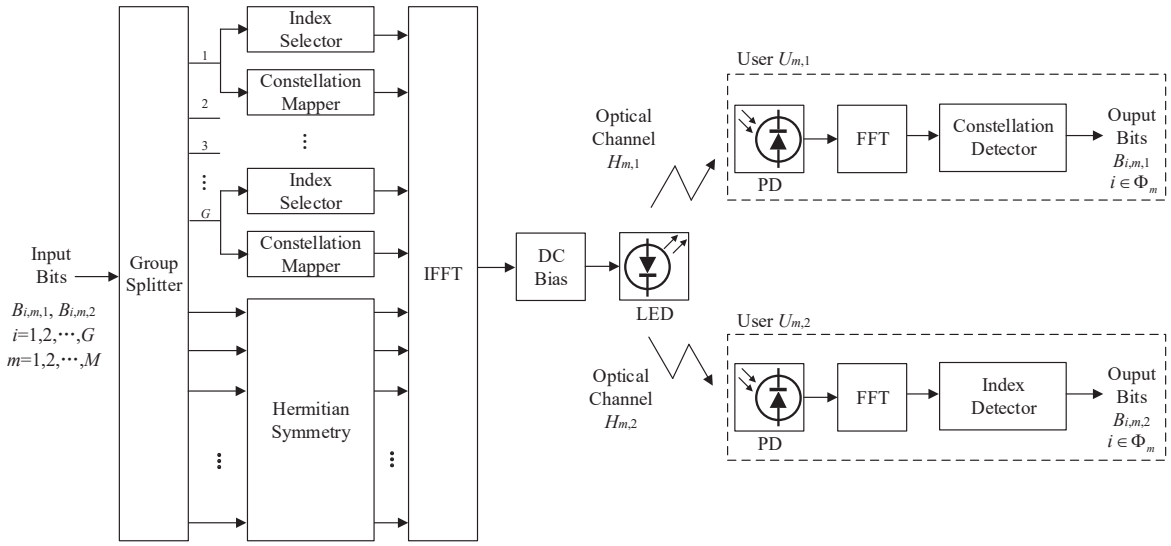


Fig. 1. The system model of the index modulation aided NOMA for VLC downlink.

the numerical simulations are carried out and the results are provided in Section IV. Finally, we conclude the paper in Section V.

Notation: Column vectors and matrices are denoted by lowercase and uppercase boldface letters; conjugate transposition, determinant, and binomial coefficient are denoted by $(\cdot)^{\mathrm{H}}$, $|\cdot|$, and $\binom{\cdot}{\cdot}$, respectively; the union and the intersection of sets are denoted by $\bigcup$ and $\bigcap$, respectively.

II. System Model

In this paper, we consider a multi-user IM-NOMA system using direct current biased optical OFDM (DCO-OFDM) [17]. The system model is shown in Fig. 1. The supported users are divided into M clusters of two, which are denoted as $U_{m,1}$ and $U_{m,2}$ $(m = 1, 2, ..., M)$.

Index modulation is also adopted in the system. The bandwidth is W and is divided into N_{F} subcarriers. Since DCO-OFDM is adopted, only $N = N_{\mathrm{F}}/2$ subcarriers can be modulated independently and the other half is generated according to the Hermitian symmetry. The independently modulated subcarriers are further divided into G groups g_i $(i = 1, 2, ..., G)$ with $L = N/G$ subcarriers in each group. Due to the principle of index modulation, the information bits can be mapped to both the constellation-domain symbols and the index-domain symbols. In each group, only K subcarriers are activated to map constellation-domain symbols. The indices of the active subcarriers can be used to transmit index-domain information. Specifically, $N_c = \binom{L}{K}$ different active index sets can be selected to transmit $\log_2(N_c)$ bits in one index-domain symbol for each subcarrier group. The optional active index sets are denoted as $\Psi_j (j = 1, 2, ..., N_c)$.

According to [18], the channel impulse response (CIR) of the indoor line-of-sight (LOS) optical channel for the q-th user in the m-th cluster can be formulated as

$$h_{m,q}(t) = \frac{(l+1)A_{\mathrm{R}}}{2\pi d_{m,q}^2} \cos^l(\phi_{m,q}) \cos(\theta_{m,q}) \delta(t - \frac{d_{m,q}}{c_l}), \quad 0 \le \theta_{m,t} \le \Theta_{1/2}, \tag{1}$$

where $\phi_{m,q}$, $\theta_{m,q}$, and $d_{m,q}$ denote the angle of irradiance, the angle of incidence, and the distance between the LED and the photo-detector (PD) of the q-th user in the m-th cluster, respectively. A_{R} and $\Theta_{1/2}$ denote the area and the field of vision (FOV) semiangle of the PD, respectively. $\delta(\cdot)$ represents the Dirac delta function and c_l represents the speed of light. l is the Lambertian mode number [19], and is given as

$$l = -\frac{\ln 2}{\ln(\cos \Phi_{1/2})}, \tag{2}$$

where $\Phi_{1/2}$ denotes the half-intensity radiation angle of the LED. A two-user example is illustrated in Fig. 2. Thus, the channel DC gain can be calculated as

$$\begin{aligned} H_{m,q} &= \int_{-\infty}^{\infty} h_{m,q}(t)\ \mathrm{d}t \\ &= \begin{cases} \frac{(l+1)A_{\mathrm{R}}}{2\pi d_{m,q}^2} \cos^l(\phi_{m,q}) \cos(\theta_{m,q}), & 0 \le \theta_{m,q} \le \Theta_{1/2} \\ 0, & \text{elsewhere.} \end{cases} \end{aligned} \tag{3}$$

Thus, the transmission functions of the users in the m-th cluster are given as

$$\mathbf{y}_{m,1} = \gamma \sqrt{P} H_{m,1} \mathbf{x} + \mathbf{w}_{m,1}, \tag{4}$$

and

$$\mathbf{y}_{m,2} = \gamma \sqrt{P} H_{m,2} \mathbf{x} + \mathbf{w}_{m,2}, \tag{5}$$

Authorized licensed use limited to: Tsinghua University. Downloaded on September 27,2020 at 12:50:31 UTC from IEEE Xplore. Restrictions apply.

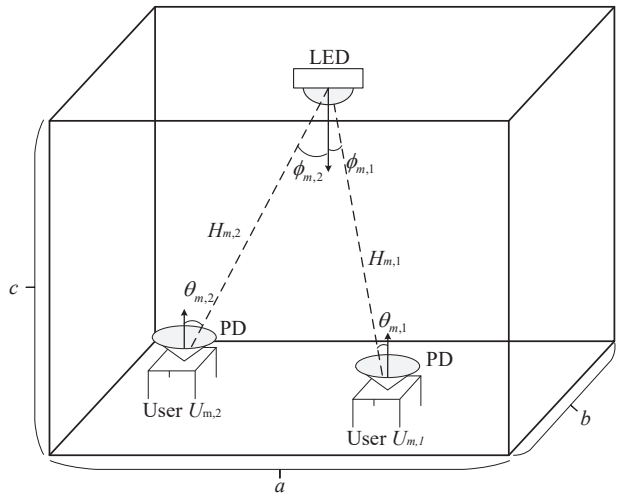


Fig. 2. Illustration of geometry of the indoor VLC downlink system.

where $\mathbf{y}_{m,1}$, $\mathbf{w}_{m,1}$, $H_{m,1}$, $\mathbf{y}_{m,2}$, $\mathbf{w}_{m,2}$, and $H_{m,2}$ denote the received signals, the noises, and the optical channel gains of user $U_{m,1}$ and $U_{m,2}$, respectively. $\mathbf{x}$ is the transmitted symbols at the LED, P denotes the total transmit electrical power, and γ represents the responsivity of the PDs.

III. Proposed IM-NOMA Scheme

A. Transmitter Design

In the proposed IM-NOMA scheme for VLC, one or more subcarrier groups are allocated to each user cluster according to the user requirements. We denote the subcarrier groups allocated to the m-th user cluster as $\Omega_m (m = 1, 2, ..., M)$. Thus, we have

$$\bigcup_{m=1}^{M} \Omega_m = \{g_1, g_2, ..., g_G\}, \tag{6}$$

and

$$\Omega_{m_1} \bigcap \Omega_{m_2} = \varnothing, \tag{7}$$

where $m_1, m_2 \in [1, M], m_1 \neq m_2$.

In the subcarrier group g_i, which is allocated to the m-th user cluster, the information bits for the two users are denoted as $B_{i,m,1}$ and $B_{i,m,2}$. In the proposed scheme, $B_{i,m,1}$ is mapped to the constellation-domain symbols, while $B_{i,m,2}$ is mapped to the index of the active subcarriers. Therefore, the data information for the two users in each cluster is conveyed in the same time and frequency resources, and there is no intra-cluster interference between the two users.

Then, the other half of the frequency-domain OFDM symbols are generated by Hermitian symmetry, and the inverse fast Fourier transform (IFFT) is applied to derive the time-domain OFDM signals. Finally, the direct current bias is added and the DCO-OFDM signals are transmitted through the optical channel.

B. Receiver Design

At the receiver side, each user is equipped with a PD to detect the optical signals. After applying the fast Fourier transform (FFT), one user in each cluster can use a simple index detector, such as maximum ratio combining (MRC), to estimate the required index-domain information. It is more suitable for the IoT devices, which have limited computing capacities and low data rate requirements. The other user in the same cluster is equipped with a more complicated constellation detector to demodulate the constellation symbols, which is more suitable for the mobile devices such as smartphones and computers that require high communication data rate. State-of-the-art user pairing techniques can be used to facilitate the user pairing.

It is worth noting that in the proposed IM-NOMA scheme, there is no need to apply SIC as in conventional NOMA schemes, since there is no intra-cluster interference between users. SIC requires the near user to decode the information intended for the far user first and subtract it from the received signals, which involves a lot of computation. Thus, the proposed IM-NOMA scheme can simplify the detector and reduce the computational complexity.

C. Achievable Sum Rate Analysis for the Physical Layer Downlink

In this subsection, the achievable sum rate of the proposed scheme is analyzed through mutual information analysis. A closed-form approximation is derived for the two-user scenario, and its principle can be easily extended to the multi-user scenarios as well. Without loss of generality, we omit the subscript m in order to express the analysis procedure more concisely.

Due to the chain rule of mutual information, the total mutual information conveyed by the IM-NOMA symbols for the i-th user is given by

$$I(\mathbf{x}; \mathbf{y}_i) = I(\mathbf{x}^{\mathrm{s}}; \mathbf{y}_i | \mathbf{x}^{\mathrm{c}}) + I(\mathbf{x}^{\mathrm{c}}; \mathbf{y}_i), \tag{8}$$

where $\mathbf{x}^{\mathrm{c}}$ denotes the index-domain symbols and $\mathbf{x}^{\mathrm{s}}$ denotes the constellation-domain symbols. $I(\mathbf{x}^{\mathrm{s}}; \mathbf{y}_i | \mathbf{x}^{\mathrm{c}})$ and $I(\mathbf{x}^{\mathrm{c}}; \mathbf{y}_i)$ represent the mutual information conveyed by the constellation-domain and index-domain symbols, respectively.

In the proposed IM-NOMA scheme, only the mutual information conveyed by the constellation-domain symbols is useful for the first user, which can be given as

$$I(\mathbf{x}^{\mathrm{s}}; \mathbf{y}_1 | \mathbf{x}^{\mathrm{c}}) = \sum_{j=1}^{N_c} \Pr(\mathbf{x}^{\mathrm{c}} = \Psi_{\mathrm{j}}) \mathrm{I}(\mathbf{x}^{\mathrm{s}}; \mathbf{y}_1 | \mathbf{x}^{\mathrm{c}} = \Psi_{\mathrm{j}}), \tag{9}$$

where $\Pr(\mathbf{x}^{\mathrm{c}} = \Psi_{\mathrm{j}})$ denotes the probability of transmitting the index-domain symbol Ψ_j. Supposing the index-domain symbols are selected with equal probability and the power is allocated equally for each subcarrier, the mutual information

Authorized licensed use limited to: Tsinghua University. Downloaded on September 27,2020 at 12:50:31 UTC from IEEE Xplore. Restrictions apply.

under Gaussian inputs for the first user can be further given as

$$\begin{aligned} I(\mathbf{x}^{\mathrm{s}};\mathbf{y}_1|\mathbf{x}^{\mathrm{c}}) &= \frac{1}{N_c}\sum_{j=1}^{N_c}\sum_{i\in\Psi_j}\log_2(1+\frac{\gamma^2{H_1}^2P}{N_0W/GL}) \\ &= \frac{K}{L}\sum_{i=1}^{L}\log_2(1+\frac{\gamma^2{H_1}^2P/GK}{N_0W/GL}) \\ &= K\log_2(1+\frac{\gamma^2{H_1}^2PL}{KN_0W}), \end{aligned} \tag{10}$$

where N_0 denotes the noise power density. Then, the achievable rate for the first user can be derived as

$$\begin{aligned} R_1 &= G\times\frac{W}{2N}\times I(\mathbf{x}^{\mathrm{s}};\mathbf{y}_1|\mathbf{x}^{\mathrm{c}}) \\ &= \frac{WK}{2L}\log_2(1+\frac{\gamma^2{H_1}^2PL}{KN_0W}). \end{aligned} \tag{11}$$

For the second user, the data information is conveyed by the index-domain symbols, the mutual information of which is given as

$$\begin{aligned} I(\mathbf{x}^{\mathrm{c}};\mathbf{y}_2) = \frac{1}{N_c}\sum_{j=1}^{N_c}\int_{\mathbf{y}_2} f(\mathbf{y}_2|\mathbf{x}^{\mathrm{c}}=\Psi_j) \\ \times\log_2(\frac{f(\mathbf{y}_2|\mathbf{x}^{\mathrm{c}}=\Psi_j)}{f(\mathbf{y}_2)})\mathrm{d}\mathbf{y}_2, \end{aligned} \tag{12}$$

where $f(\mathbf{y}_2|\mathbf{x}^{\mathrm{c}}=\Psi_j)$ and $f(\mathbf{y}_2)$ denote the conditional probability density function and the probability density function, respectively. These two functions can be further expressed as

$$f(\mathbf{y}_2|\mathbf{x}^{\mathrm{c}}=\Psi_j) = \frac{1}{\pi^L|\Sigma_j|}\exp\left(\mathbf{y}_2^{\mathrm{H}}\Sigma_j^{-1}\mathbf{y}_2\right), \tag{13}$$

and

$$f(\mathbf{y}_2) = \frac{1}{N_c}\sum_{j=1}^{N_c} f(\mathbf{y}_2|\mathbf{x}^{\mathrm{c}}=\Psi_j), \tag{14}$$

where $\Sigma_j(j=1,2,...,N_c)$ is the covariance matrix of $\mathbf{y}_2$ when the transmitted index-domain symbol is $\mathbf{x}^{\mathrm{c}}=\Psi_j$. Supposing the transmitted symbols are independent with the noise, Σ_j is a diagonal matrix according to the transmission equation in (5). According to [20], the mutual information in (12) has no closed-form expression, which can be divided into two parts

$$I(\mathbf{x}^{\mathrm{c}};\mathbf{y}_2) = \frac{1}{N_c}\sum_{j=1}^{N_c}(\Xi_{j,1}-\Xi_{j,2}). \tag{15}$$

The first part can be calculated as

$$\begin{aligned} \Xi_{j,1} &= \int_{\mathbf{y}_2} f(\mathbf{y}_2|\mathbf{x}^{\mathrm{c}}=\Psi_j)\times\log_2(f(\mathbf{y}_2|\mathbf{x}^{\mathrm{c}}=\Psi_j))\mathrm{d}\mathbf{y}_2 \\ &= -L\log_2(\pi e)-\log_2(|\Sigma_j|), \end{aligned} \tag{16}$$

and the second part can be expressed as

$$\Xi_{j,2} = \int_{\mathbf{y}_2} f(\mathbf{y}_2|\mathbf{x}^{\mathrm{c}}=\Psi_j)\times\log_2(\frac{1}{N_c}\sum_{t=1}^{N_c} f(\mathbf{y}_2|\mathbf{x}^{\mathrm{c}}=\Psi_t))\mathrm{d}\mathbf{y}_2. \tag{17}$$

Due to the concavity of the $\log_2(\cdot)$ function, Jensen's inequality [21] can be utilized to derive the upper bound of (17), which is expressed as

$$\Xi_{j,2} \le \log_2\left(\frac{1}{N_c}\sum_{t=1}^{N_c}\int_{\mathbf{y}_2} f(\mathbf{y}_2|\mathbf{x}^{\mathrm{c}}=\Psi_j)\times f(\mathbf{y}_2|\mathbf{x}^{\mathrm{c}}=\Psi_t)d\mathbf{y}_2\right). \tag{18}$$

After substituting the conditional probability density function in (13), the upper bound can be further derived as

$$\begin{aligned} \Xi_{j,2} &\le \log_2(\frac{1}{N_c\pi^L}\sum_{t=1}^{N_c}\frac{1}{|\Sigma_n||\Sigma_t||\Sigma_j^{-1}+\Sigma_t^{-1}|} \\ &\int_{\mathbf{y}_2}\frac{1}{\pi^L|(\Sigma_j^{-1}+\Sigma_t^{-1})^{-1}|}\exp\left(\mathbf{y}_2^H(\Sigma_n^{-1}+\Sigma_t^{-1})\mathbf{y}_2\right)d\mathbf{y}_2) \\ &= -L\log_2(\pi)+\log_2\left(\frac{1}{N_c}\sum_{t=1}^{N_c}\frac{1}{|\Sigma_j+\Sigma_t|}\right). \end{aligned} \tag{19}$$

Therefore, the lower bound of the mutual information for the second user is yielded as

$$I(\mathbf{x}^{\mathrm{c}};\mathbf{y}_2) \ge \log_2\left(\frac{N_c}{e^L}\right)-\frac{1}{N_c}\sum_{j=1}^{N_c}\log_2\left(\sum_{t=1}^{N_c}\frac{|\Sigma_j|}{|\Sigma_j+\Sigma_t|}\right). \tag{20}$$

It is worth noting that the right-hand side of (20) approaches $-L\log_2(e/2)$ and $\log_2(N_c)-L\log_2(e/2)$ at low and high signal to noise ratio (SNR) regions, respectively. However, the true value of the mutual information in (12) approaches 0 and $\log_2(N_c)$, respectively. Thus, we apply a constant shift $L\log_2(e/2)$ to the right-hand side of (20) to obtain a closed-form approximation, which is

$$I(\mathbf{x}^{\mathrm{c}};\mathbf{y}_2) \approx \log_2\left(\frac{N_c}{2^L}\right)-\frac{1}{N_c}\sum_{j=1}^{N_c}\log_2\left(\sum_{t=1}^{N_c}\frac{|\Sigma_j|}{|\Sigma_j+\Sigma_t|}\right). \tag{21}$$

Thus, the closed-form approximation of the data rate of the second user is further derived as

$$\begin{aligned} R_2 &= G\times\frac{W}{2N}\times I(\mathbf{x}^{\mathrm{c}};\mathbf{y}_2) \\ &\approx \frac{W}{2L}\log_2\left(\frac{N_c}{2^L}\right)-\frac{W}{2LN_c}\sum_{j=1}^{N_c}\log_2\left(\sum_{t=1}^{N_c}\frac{|\Sigma_j|}{|\Sigma_j+\Sigma_t|}\right). \end{aligned} \tag{22}$$

Authorized licensed use limited to: Tsinghua University. Downloaded on September 27,2020 at 12:50:31 UTC from IEEE Xplore. Restrictions apply.

TABLE I
PARAMETERS FOR SIMULATION

Parameter	Explication	Value
l	Lambertian mode number of the LED	1
A_{R}	Area of the PDs	1 cm^2
$\Theta_{1/2}$	FOV of the PDs	60°
γ	Responsivity of the PDs	0.25 A/W
N_0	Noise power density at the PDs	-180 dBm

As a result, the closed-form approximation of the achievable sum rate of the two users can be finally derived as

$$\begin{aligned} R =& R_1 + R_2 \\ \approx& \frac{WK}{2L}\log_2(1+\frac{\gamma^2 {H_1}^2 PL}{KN_0W})+\frac{W}{2L}\log_2\left(\frac{N_c}{2^L}\right) \\ &- \frac{W}{2LN_c}\sum_{j=1}^{N_c}\log_2\left(\sum_{t=1}^{N_c}\frac{|\Sigma_j|}{|\Sigma_j+\Sigma_t|}\right). \end{aligned} \tag{23}$$

IV. SIMULATION RESULTS

We consider an indoor VLC system in an empty cubic room with size $a = 5$ m, $b = 5$ m, and $c = 3$ m, which is illustrated in Fig. 2. The LED is placed in the center of the ceiling $(2.5, 2.5, 3)$ pointing straight down. Two users are supported in the VLC system, one is located in the center of the room $(2.5, 2.5, 0.7)$ and the other is located around the corner $(0.7, 0.7, 0.7)$. The PDs of both users are pointing straight up. The parameters of the LED and PDs are summarized in Table I [22], [23]. Thus, the channel gains are calculated as $H_1 = -52$ dB and $H_2 = -59$ dB. The bandwidth is $W = 20$ MHz, which is divided into $N_{\mathrm{F}} = 128$ subcarriers. The subcarriers form $G = 4$ groups, and $L = N_{\mathrm{F}}/(2G) = 16$ subcarriers can be selected to transmit constellation symbols in each group.

In Fig. 3, the achievable sum rate of the proposed IM-NOMA is investigated with different numbers of activated subcarriers K and total transmit electrical power P. The exact values of the achievable sum rates are represented by the solid lines. The closed-form lower bounds and approximations (23) are depicted by the dash-dotted lines and the dotted lines, respectively. It can be seen that the derived lower bounds can track the trends of the exact values very well and after applying the constant shift, the closed-form approximations are very close to the exact values, which validates the effectiveness of the proposed closed-form approximations. It can also be seen that the achievable sum rates rise with the increase of the number of the activated subcarriers K. It is mainly because that by activating more subcarriers, the increased data rate of the first user is larger than the decreased data rate of the second user.

We further compare the achievable sum rates of the proposed IM-NOMA with the conventional NOMA scheme [10] and orthogonal frequency division multiple access (OFDMA) scheme [24] in Fig. 4. In the OFDMA scheme, two users are

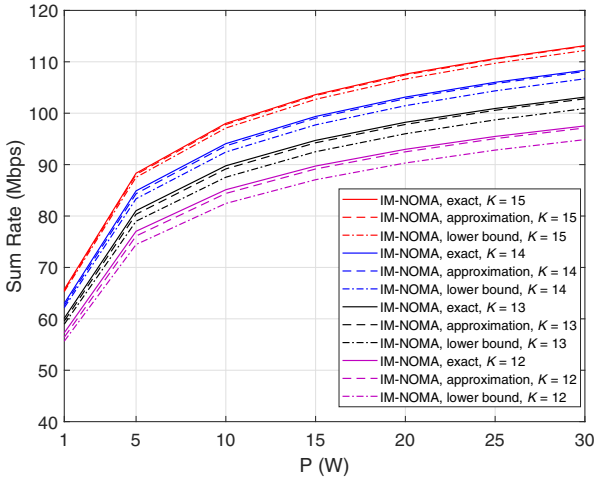


Fig. 3. Comparisons of the achievable sum rates of the proposed IM-NOMA with different numbers of activated subcarriers K.

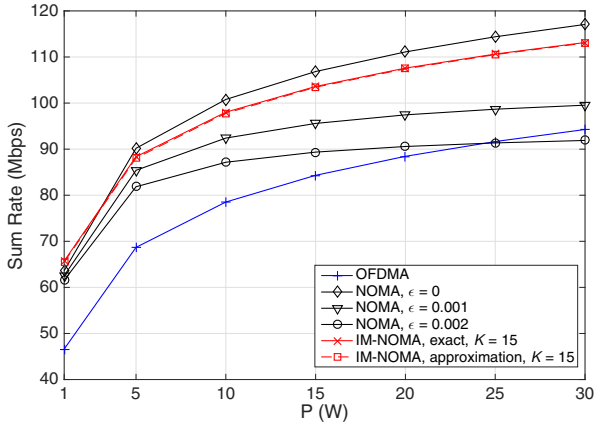


Fig. 4. Comparisons of the achievable sum rates of the proposed IM-NOMA and conventional multiple access schemes with different transmit power P.

allocated with an equal number of orthogonal subcarriers. In the conventional NOMA scheme, $0.8P$ is allocated to the second user and $0.2P$ is allocated to the first user. Thus, the second user can decode the desired information by regarding the signal for the first user as interference. And the first user utilizes SIC to remove the interference caused by the second user. We use ϵ to denote the cancellation error term [25] that represents the remaining portion of the canceled signals by SIC. It can be seen that the proposed IM-NOMA achieves much better sum rate than the OFDMA scheme, which is mainly because of the non-orthogonal resource allocation. The conventional NOMA enjoys higher achievable sum rate than IM-NOMA with perfect SIC, however, the sum rate decreases a lot even with slightly imperfect SIC. It can be seen that the proposed IM-NOMA obtains much higher sum rates than the conventional NOMA with imperfect SIC $\epsilon = 0.001$ and $\epsilon = 0.002$.

Authorized licensed use limited to: Tsinghua University. Downloaded on September 27,2020 at 12:50:31 UTC from IEEE Xplore. Restrictions apply.

V. Conclusion

In this paper, a novel index modulation aided NOMA scheme has been proposed for VLC, which conveys information for different users through index-domain and constellation-domain symbols with the aid of index modulation. The intra-cluster interference is canceled completely and the complicated SIC is avoided, then low computational complexity can be achieved at the user side. The achievable sum rate of the proposed IM-NOMA has been analyzed and a closed-form approximation of the achievable sum rate has been derived. The effectiveness of the proposed approximation and the superior performance compared with the conventional multiple access schemes are validated through simulations.

Acknowledgement

This work is based upon research supported by the National Natural Science Foundation of China (Grant No. 61871255), the National Key Research and Development Program of China (Grant No. 2017YFE0113300), the Natural Science Foundation of Guangdong Province (Grant No. 2015A030312006), the Beijing National Research Center for Information Science and Technology Program (Grant No. BNR2019TD01001 and BNR2019RC01015), and the Tsinghua University Tutor Research Fund.

References

[1] Z. Ghassemlooy, S. Arnon, M. Uysal, Z. Xu, and J. Cheng, "Emerging optical wireless communications-advances and challenges," *IEEE J. Sel. Areas Commun.*, vol. 33, no. 9, pp. 1738–1749, Sep. 2015.

[2] P. H. Pathak, X. Feng, P. Hu, and P. Mohapatra, "Visible light communication, networking, and sensing: A survey, potential and challenges," *IEEE Commun. Surveys Tuts.*, vol. 17, no. 4, pp. 2047–2077, Sep. 2015.

[3] X. Huang, F. Yang, C. Pan, and J. Song, "Advanced ADO-OFDM with adaptive subcarrier assignment and optimized power allocation," *IEEE Wireless Commun. Lett.*, pp. 1–1, Apr. 2019.

[4] T. Wang, F. Yang, L. Cheng, and J. Song, "Spectral-efficient generalized spatial modulation based hybrid dimming scheme with LACO-OFDM in VLC," *IEEE Access*, vol. 6, pp. 41 153–41 162, Jun. 2018.

[5] W. Ding, F. Yang, H. Yang, J. Wang, X. Wang, X. Zhang, and J. Song, "A hybrid power line and visible light communication system for indoor hospital applications," *Computers in Industry*, vol. 68, pp. 170–178, Feb. 2015.

[6] Y. Sun, F. Yang, and J. Gao, "Comparison of hybrid optical modulation schemes for visible light communication," *IEEE Photon. J.*, vol. 9, no. 3, pp. 1–13, Jun. 2017.

[7] F. Yang, J. Gao, and S. Liu, "Novel visible light communication approach based on hybrid OOK and ACO-OFDM," *IEEE Photon. Technol. Lett.*, vol. 28, no. 14, pp. 1585–1588, Jul. 2016.

[8] E. Basar, M. Wen, R. Mesleh, M. D. Renzo, Y. Xiao, and H. Haas, "Index modulation techniques for next-generation wireless networks," *IEEE Access*, vol. 5, pp. 16 693–16 746, 2017.

[9] E. Basar, "Index modulation techniques for 5G wireless networks," *IEEE Commun. Mag.*, vol. 54, no. 7, pp. 168–175, Jul. 2016.

[10] R. C. Kizilirmak, C. R. Rowell, and M. Uysal, "Non-orthogonal multiple access (NOMA) for indoor visible light communications," in *2015 4th International Workshop on Optical Wireless Communications (IWOW)*, Sep. 2015, pp. 98–101.

[11] Z. Ding, Z. Yang, P. Fan, and H. V. Poor, "On the performance of non-orthogonal multiple access in 5G systems with randomly deployed users," *IEEE Signal Process. Lett.*, vol. 21, no. 12, pp. 1501–1505, Dec. 2014.

[12] Z. Ding, Y. Liu, J. Choi, Q. Sun, M. Elkashlan, C. I, and H. V. Poor, "Application of non-orthogonal multiple access in LTE and 5G networks," *IEEE Commun. Mag.*, vol. 55, no. 2, pp. 185–191, Feb. 2017.

[13] C. Chen, W. Zhong, H. Yang, and P. Du, "On the performance of MIMO-NOMA-based visible light communication systems," *IEEE Photon. Technol. Lett.*, vol. 30, no. 4, pp. 307–310, Feb. 2018.

[14] X. Zhang, Q. Gao, C. Gong, and Z. Xu, "User grouping and power allocation for NOMA visible light communication multi-cell networks," *IEEE Commun. Lett.*, vol. 21, no. 4, pp. 777–780, Apr. 2017.

[15] Y. Fu, Y. Hong, L. Chen, and C. W. Sung, "Enhanced power allocation for sum rate maximization in OFDM-NOMA VLC systems," *IEEE Photon. Technol. Lett.*, vol. 30, no. 13, pp. 1218–1221, Jul. 2018.

[16] T. Wang, J. Tan, W. Ding, Y. Zhang, F. Yang, J. Song, and Z. Han, "Intercommunity detection scheme for social Internet of Things: Compressive sensing over graphs approach," *IEEE Internet Things J.*, vol. 5, no. 6, pp. 4550–4557, Dec. 2018.

[17] J. B. Carruthers and J. M. Kahn, "Multiple-subcarrier modulation for non-directed wireless infrared communication," *IEEE J. Sel. Areas Commun.*, vol. 14, no. 3, pp. 538–546, Apr. 1996.

[18] K. Lee, H. Park, and J. R. Barry, "Indoor channel characteristics for visible light communications," *IEEE Commun. Lett.*, vol. 15, no. 2, pp. 217–219, Feb. 2011.

[19] F. Miramirkhani and M. Uysal, "Channel modeling and characterization for visible light communications," *IEEE Photon. J.*, vol. 7, no. 6, pp. 1–16, Dec. 2015.

[20] M. Wen, X. Cheng, M. Ma, B. Jiao, and H. V. Poor, "On the achievable rate of OFDM with index modulation," *IEEE Trans. Signal Process.*, vol. 64, no. 8, pp. 1919–1932, Apr. 2016.

[21] L. He, J. Wang, and J. Song, "Spectral-efficient analog precoding for generalized spatial modulation aided mmWave MIMO," *IEEE Trans. Veh. Technol.*, vol. 66, no. 10, pp. 9598–9602, Oct. 2017.

[22] T. Komine and M. Nakagawa, "Fundamental analysis for visible-light communication system using LED lights," *IEEE Trans. Consum. Electron.*, vol. 50, no. 1, pp. 100–107, Feb. 2004.

[23] I. Stefan, H. Burchardt, and H. Haas, "Area spectral efficiency performance comparison between VLC and RF femtocell networks," in *2013 IEEE International Conference on Communications (ICC)*, Jun. 2013, pp. 3825–3829.

[24] B. Lin, X. Tang, Z. Ghassemlooy, C. Lin, and Y. Li, "Experimental demonstration of an indoor VLC positioning system based on OFDMA," *IEEE Photon. J.*, vol. 9, no. 2, pp. 1–9, Apr. 2017.

[25] J. G. Andrews and T. H. Meng, "Optimum power control for successive interference cancellation with imperfect channel estimation," *IEEE Trans. Wireless Commun.*, vol. 2, no. 2, pp. 375–383, Mar. 2003.

Authorized licensed use limited to: Tsinghua University. Downloaded on September 27,2020 at 12:50:31 UTC from IEEE Xplore. Restrictions apply.